UDK 678.84
Original scientific article/Izvirni znanstveni članek

ISSN 1580-2949
MTAEC9, 49(1)3(2015)

BORON-DOPED HYDROGENATED AMORPHOUS SEMICONDUCTOR MEMS

Z BOROM DOPIRANI HIDROGENIRANI AMORFNI POLPREVODNIK MEMS

Margarita Galindo[1], Carlos Zúñiga[2], Rodolfo Palomino-Merino[1], Francisco López[3], Wilfrido Calleja[2], Javier de la Hidalga[2], Victor M. Castaño[4]

[1]Facultad de Ciencias Físico-Matemáticas, Benemérita Universidad Autónoma de Puebla, Av. San Claudio y 18 Sur, Col. San Manuel, Ciudad Universitaria, 72570 Puebla, Mexico
[2]Instituto Nacional de Astrofísica, Óptica y Electrónica (INAOE), Luis E Erro # 1, Santa María Tonantzintla, Puebla, Mexico
[3]Facultad de Ciencias de la Electrónica, Benemérita Universidad Autónoma de Puebla, Av. San Claudio y 18 Sur, Col. San Manuel, Ciudad Universitaria, 72570 Puebla, Mexico
[4]Centro de Fisica Aplicada y Tecnologia Avanzada, Campus Juriquilla, Queretaro, Mexico (on sabbatical leave at CIATEQ-Queretaro)
meneses@unam.mx

Prejem rokopisa – received: 2013-01-28; sprejem za objavo – accepted for publication: 2014-01-17

A micromachining process for the fabrication of micro-electro-mechanical systems (MEMSs), using both boron-doped silicon and silicon-germanium amorphous films (a-SiB:H and a-Si0.50Ge0.50B:H) prepared with plasma-enhanced chemical vapor deposition (PECVD), at 110 kHz, 300 °C and a low pressure ($8 \cdot 10^{-4}$ mbar) is presented. These MEMSs were fabricated using a surface micromachining technology with wet and dry etching. The microstructures made of a-Si0.50Ge0.50B:H and a-SiB:H, with a structural single layer with a thickness of 1 μm were fabricated. Diamond, ring, V and Vernier-beam structures were included in the MEMS process. We found optical gaps of 1.55 eV and 0.97 eV for the a-SiB:H and a-Si0.50Ge0.50B:H films, respectively. We varied the boron doping concentration for the a-Si0.50Ge0.50B:H samples, causing a decrease in the resistance from 6.84 MΩ to 0.2 MΩ. A compressive stress of 13.44 MPa was obtained for the diamond-type microstructures of a-SiB:H. An improved mechanical stability and lateral definition were obtained for the a-Si0.50Ge0.50B:H microstructures, with a compressive stress of 10.66 MPa. These microstructures showed excellent characteristics for their integration in the production of MEMSs.

Keywords: MEMS, Vernier beam, diamond-type structure, amorphous silicon, amorphous silicon germanium, PECVD

Predstavljen je postopek mikroobdelave pri izdelavi mikroelektromehanskega sistema (MEMS) z borom dopiranih silicijevih in silicij-germanijevih amorfnih tankih plasti (a-SiB:H in a-Si0,50Ge0,50B:H), izdelanih s kemijskim postopkom nanašanja iz parne faze v plazmi (PECVD) pri 110 kHz in 300 °C pri tlaku $8 \cdot 10^{-4}$ mbar. MEMS so bili izdelani s tehnologijo mikroobdelave površine z mokrim in suhim jedkanjem. Izdelane so bile mikrostrukture iz a-Si0,50Ge0,50B:H in a-SiB:H, ki sestojijo iz ene plasti debeline 1 μm. V proces MEMS so bile vključene diamantne, obročaste, V in Vernierjeve stebraste strukture. V plasti a-SiB:H in a-Si0,50Ge0,50B:H smo našli optične vrzeli pri 1,55 eV in 0,97 eV. Spreminjanje koncentracije dopiranega bora v vzorcu a-Si0,50Ge0,50B:H je pripeljalo do zmanjšanja upornosti od 6,84 MΩ na 0,2 MΩ. Tlačna napetost 13,44 MPa je bila dosežena v diamantni mikrostrukturi a-SiB:H. Izboljšana mehanska stabilnost je bila dobljena pri mikrostrukturi a-Si0,50Ge0,50B:H s tlačno napetostjo 10,66 MPa. Te mikrostrukture kažejo odlične lastnosti za njihovo vključitev pri izdelavi MEMS.

Ključne besede: MEMS, Vernierjev steber, diamantna struktura, amorfni silicij, amorfni silicij-germanij, PECVD

1 INTRODUCTION

Recent advances in micromachining technologies related with the manufacturing of micro-electro-mechanical systems (MEMSs) made it necessary to investigate new materials to be used for the fabrication of modern devices[1–3]. Some materials can be deposited at the temperatures that are low enough (below 300 °C) to remain unaffected during a regular process involving a thermal load in the production of any complex microelectronics, for instance, when sensors and/or actuators (accelerometers, anemometers, gyroscopes, thermal devices, RF-transmitters, photodetectors, optical modulators, micromirrors[4–8]) must be integrated using a complementary metal-oxide semiconductor (CMOS) technology[9,10]. A variety of materials, such as amorphous Si (a-Si), amorphous Ge (a-Ge) and the amorphous Si-Ge alloy (a-SiGe), can be nowadays deposited onto different substrates, using plasma-enhanced chemical vapor deposition (PECVD)[11–13]. Currently, these materials are attracting the attention because their electrical and mechanical properties are suitable for manufacturing microstructures.

The a-SiGe films were developed mainly for the applications in optoelectronic devices. The optical band gap of an amorphous material is determined with the content ratio of Si/Ge in the film. In general, optical, electrical and mechanical properties can be varied according to the type and ratio of the introduced gases during the deposition. In particular, the mechanical properties provide a new property of amorphous semiconductors for fabricating microstructures.

On the other hand, most of the microstructures for MEMSs are made with polysilicon (i.e., polycrystalline silicon); however, this material is deposited and doped at 650 °C and 900 °C, respectively, and this affects the

thermal budget of the process. Thus, on the basis of our knowledge of the PolyMEMSV process, we fabricated microstructures using a-SiGe films. We used this material because a-SiGe films, deposited at 300 °C, can show properties similar to those presented by polysilicon processed at much higher temperatures. Furthermore, the a-SiGe properties such as Young's modulus, bond content, thickness, resistivity and optical gap can be varied with the deposition conditions (frequency, pressure, temperature and gas-flow rate). It was found[14] that Si-Ge forms polymeric chains that do not alter at all the procedure explained in this article.

1.1 Mechanical structures for monitoring mechanical stress

One of the main problems in manufacturing surface microstructures is the presence of residual stresses. Residual stresses ($\sigma_i = E\varepsilon$) are internal mechanical forces that act on an isotropic material without the applications of external forces or temperature gradients. Residual stresses lead to mechanical deformations (ε) in the materials, resulting in fractional changes in the dimensions (linear, surface or volume)[12,13].

In order to develop a microsystem technology, we must include the structures for monitoring the efforts and residual stress on the film so that we are able to observe the presence of mechanical stresses due to the deformation. The presence of a mechanical stress causes an unpredictable behavior in static or dynamic structures. A bridge-type structure (clamped-clamped beam), under a compressive stress, presents a deformation along its structure when it is released (buckling). The critical deformation ε_{cr} can be estimated using Euler equation 1 for a beam with the critical length L_{cr}, as shown in **Figure 1**:

$$\varepsilon_{cr} = \frac{\pi^2}{12L_{cr}^2}(4D_z^2 + 4h^2) \qquad (1)$$

In the above equation h is the thickness of the beam, L_{cr} is the critical length of the beam and D_z is the strain amplitude.

1.2 Young's modulus

Young's modulus is a measure of the stiffness of an elastic material. The residual stress (σ_i) is directly proportional to Young's modulus; therefore, a higher Young's modulus corresponds to a higher stress in the material. An ANSYS® finite-element simulator was

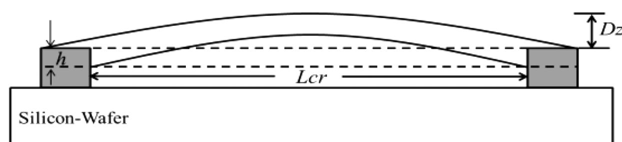

Figure 1: Bridge-type structure with a compressive stress
Slika 1: Oblika zgradbe mostička s tlačno napetostjo

used to calculate the Young's modulus for a-SiGe films[15,16] and this allowed a simulation of the dynamic behavior of the microstructure beams. A modal analysis was used to determine the first natural mode of the resonance frequency of the beam with the following conditions:

- The beam is considered as a harmonic oscillator.
- The beam is anchored at one end and free at the other end.
- The resonance frequency is proportional to the dimensions of the beam (L = 100 µm, h = 1 µm and w = 10 µm).
- The properties of the materials are: thermal-expansion coefficients, density, thermal conductivity[17,18].

The resonance frequency is a function of the dimensions and mechanical characteristics of the material:

$$F_{res} = 0.1604\sqrt{\frac{E(1-\upsilon^2)}{\rho}}\frac{h}{L^2} \qquad (2)$$

Here h is the thickness of the thin film, L is the length of the beam, ρ is the density of the material, E is Young's modulus, υ is Poisson's ratio and F_{res} is the resonance frequency of the beam[15].

1.3 Design and manufacturing of microstructures

Any PolyMEMSV chip includes passive structures such as bridge, diamond, ring, V and Vernier-beam structures acting as the monitors of the residual mechanical stress of a-SiB:H and a-$Si_{0.50}Ge_{0.50}$B:H films.

The microstructure manufacturing consists of deposition and etching of the materials, while the microstructure release is done with the chemical-etching techniques: wet and/or dry[16–23]. Surface micromachining is used to remove the material used as a sacrificial film[20–22]. In other cases, the bulk micromachining of silicon moves the wafer back[24]. Dry etching is done with the reactive-ion-etching system (RIE) or inductively coupled plasma (ICP). In contrast, wet etching uses chemical solutions, usually alkaline potassium hydroxide (KOH) and sodium hydroxide (NaOH). In the cases of both wet and dry etching, it is necessary to define the geometric patterns on the wafer to manufacture the microstructures with a photolithographic process.

The PolyMEMSV process is based on material deposition and wet and dry attacks for surface micromachining. Wet etching with potassium hydroxide and water (H_2O:KOH) at a temperature of 32 °C is used. Dry etching based on the reactive ion attack (RIE) is carried out with MicroRIE-800 from Technics Inc.[25]; CHF_3/O_2 and SF_6/O_2 gasses are used[24]. Photolithography with a positive photoresistance (ma-P1225) at 3000 r/min was applied for 30 s.[26] Our manufacturing processes are standardized to the level of a-SiGe of 1 µm on a phosphosilicate-glass (PSG) layer of 3 µm as the sacrificial material and an aluminum layer of 1 um.

1.4 Experimental setup

The experimental setup consisted of a silicon oxide (SiO_2) film as the electrical insulator, a PSG material as the sacrificial material (or a temporary mechanical support), an amorphous-film deposition and aluminum (Al) as the electrical conductor, and a crystalline silicon wafer used as the substrate. The manufacturing process is carried out in the following steps:

1. It begins with the growth of 200 nm SiO_2 films at a temperature of 1000 °C, for 30 min, in a H_2O vapor flow (**Figure 2a**).
2. A PSG sacrificial film 3 μm is deposited using an atmospheric-pressure chemical vapor deposition system (APCVD.) This film serves as a temporary mechanical support for the structures suspended. The conditions are: a temperature of 450 °C, nitrogen (N_2), silane (SiH_4) and phosphine (PH_3) flows, duration of 58 min (**Figure 2b**).

Lithography and wet etching are performed on the PSG film in order to deposit a microstructure film, applying a negative photoresistance (ma-1420) at 5000 r/min for 30 s, during an exposure time of 10 s.[25] Developed in 35 s and using a thermal annealing at 110 °C for 15 min, wet etching is performed with potassium hydroxide (KOH) to 10 % at a temperature of 32 °C for 3 min (**Figure 2c**).

The a-SiB:H and a-Si0.50Ge0.50B:H films 1 μm are deposited with the PECVD system under the following conditions: a temperature of 300 °C, a frequency of 110 kHz, a power of 500 W and a pressure of $8 \cdot 10^{-4}$ mbar. Silane (SiH_4), germane (GeH_4), hydrogen (H_2) and diborane (B_6H_4) flows are used (**Figure 2d**).

The microstructures of the a-Si1B:H and a-Si0.50Ge0.50B:H films are defined with lithography and dry etching in RIE. Sulfur tetrafluoride (SF_4) gas is used to generate the RIE plasma, with an electrical power of 200 W and the base pressure of $4 \cdot 10^{-1}$ mbar (**Figure 2e**).

Aluminum 1 μm used for electrical contacts is deposited with a physical vapor deposition system (PVD). Aluminum etching is performed using a chemical solution of H_3PO_4, CH_3COOH and HNO_3 for 7 min at 27 °C (**Figure 2f**).

The last step includes a removal of the PSG sacrificial layer to release the suspended microstructures. The technique used to release the microstructures consists of eliminating the PSG with a hydrofluoric acid solution (HF to 49 %) at room temperature for 4 min. The microstructure release is performed with 2-propanol at 62 °C, water DI at 62 °C and acetone at 62 °C to remove the residues in order to avoid a collapse (**Figure 2g**).

2 RESULTS AND DISCUSSION

The spectra of the optical absorption were measured with a UV/Vis 300 Spectronic-Unicam spectrometer[20]. The optical gap E_g of the films was extracted according to the empirical formula derived by Tauc[26–29]. **Figure 3** shows the band optical gap E_g versus the Ge content (X_g) for the films studied here. The values of the optical gap of 1.55 eV for the a-SiB:H film are also shown. As the Ge content increases from 0 to 0.25 the optical gap decreases rapidly from 1.55 eV to 1.06 eV for the a-Si0.75Ge0.25B:H films. When the Ge content $X_g > 0.5$ (a-Si0.50Ge0.50B:H) the change in the optical gap becomes slower, 0.97 eV and 0.78 eV for the a-GeB:H films.

The electrical and mechanical properties, the stress and roughness of a film are important in the fabrication of microstructures. The data obtained from the a-SiB:H thin films and the a-Si1-XGeXB:H alloy with different molar concentrations of Ge show that the optical gap

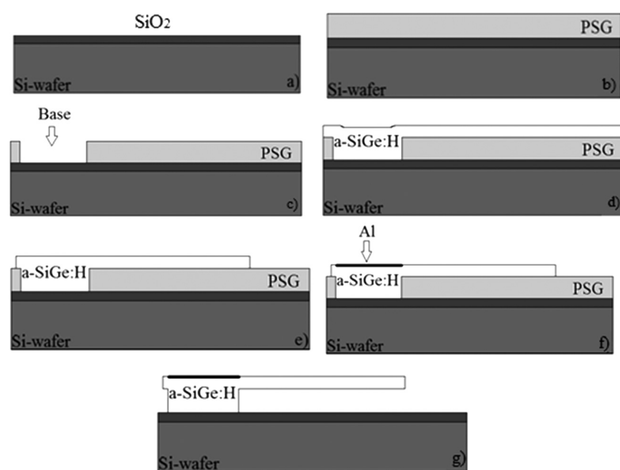

Figure 2: Sequence of the steps for the production of the microstructures of a-Si1B:H and a-Si0.50Ge0.50B:H with a thickness of 1 μm
Slika 2: Zaporedje korakov pri izdelavi mikrostrukture a-Si1B:H in a-Si0,50Ge0,50B:H debeline 1 μm

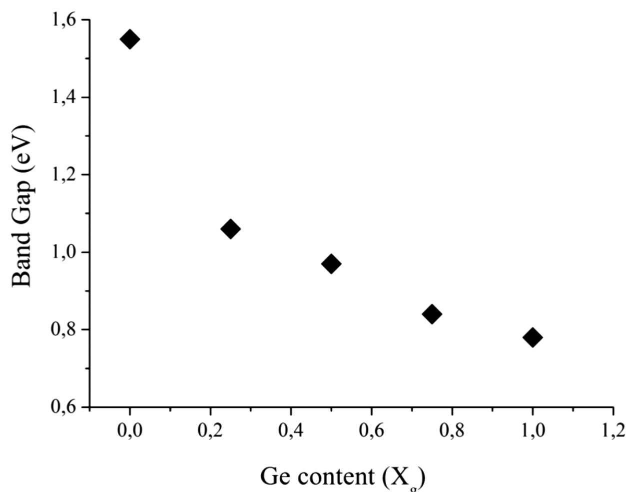

Figure 3: Band gap versus Ge content for a-Si1-XGeXB:H thin films
Slika 3: Energijska vrzel v tanki plasti a-Si1-XGeXB:H glede na vsebnost Ge

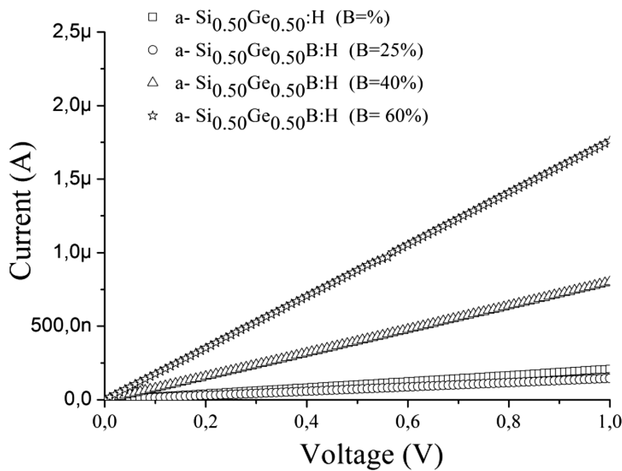

Figure 4: Current-voltage curves for the a-Si0.50Ge0.50B:H sample doped with different amounts of boron

Slika 4: Odvisnost toka od napetosti pri vzorcu a-Si0,50Ge0,50B:H, dopiranem z različnimi vsebnostmi bora

varies with the B content, but the preferential Ge incorporation in the solid phase is evident.

Figure 4 shows the current-voltage curves for the sample of a-Si0.50Ge0.50B:H doped with different amounts of boron; this graph shows that the slope of each curve changes in the range of 0.12 μA to 1.7 μA. These changes in the slope of the current-voltage curve between different samples are due to the variation in the electrical resistance of different samples. The electrical resistance decreases with the amount of boron present in the samples in the range of 6.84 MΩ to 0.514 MΩ. The a-Si0.50Ge0.50B:H sample doped with 60 % of boron has less electrical resistance. The result of an electrical characterization was obtained with a Keithley Model 2400 SourceMeter[16,30].

Figure 5 shows the resonance frequency obtained through the finite-element method using ANSYS®[16], allowing us to calculate the Young's modulus from

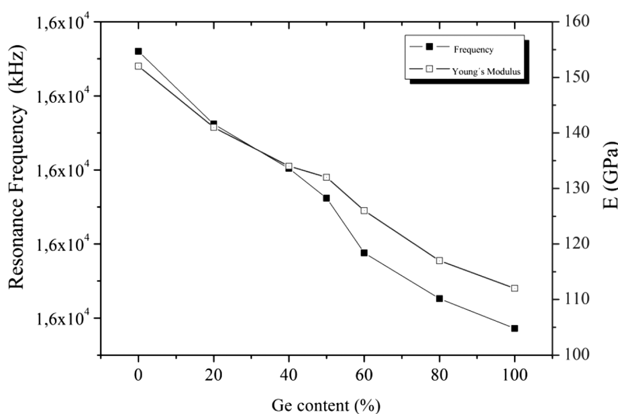

Figure 5: Resonant frequency and Young's modulus as functions of the concentration

Slika 5: Resonančna frekvenca in Youngov modul v odvisnosti od koncentracije

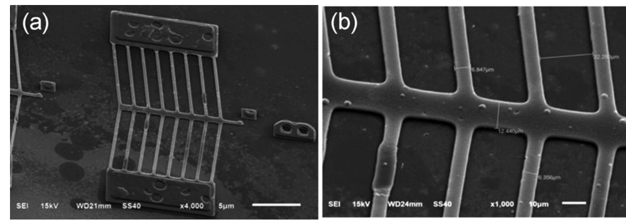

Figure 6: a) Geometric profile and b) close-to-TVM-type microstructure

Slika 6: a) Geometrijski profil in b) mikrostruktura blizu TVM

Equation 2 as a function of the germanium concentration in the bridge-type microstructure.

The analysis showed that Young's modulus can be assumed as a linear combination of the amounts of silicon and germanium in thin films.

We designed a microstructure-manufacturing process with the a-Si0.50Ge0.5B:H films deposited at the temperature of 300 °C to use it for post-processing MEMS with the CMOS technology. The SEM images were recorded at an acceleration voltage of 15 kV and in a high vacuum (HV) using a JEOL SEM model JSM-5610LV (Hitachi, Japan). The samples were placed on a specimen stub using a double-sided adhesive carbon tape.

The microstructures manufactured at a low temperature of 300 °C, with a structural level of hydrogenated amorphous silicon doped with boron (a-Si1B:H) exhibited a higher roughness on the surface and a poor definition at the edges of the structures; in addition to the chemical attack on the surface of the wafer and the structures, **Figure 6** shows SEM images of thermal microactuator chevron (TVM) type microstructures.

Additionally, when using thin films of a-Si0.50 Ge0.50B:H a direct dependence on the roughness and the definition of the edge is observed, while others do not show lateral etching on the structures or on the wafer. **Figure 7** shows the profiles of thermal bimorph micro-actuator (TBA) type microstructures manufactured with the a-Si0.50Ge0.50B:H films including a structural layer.

The microstructures of a-SiB:H and a-Si0.50Ge0.50 B:H show the presence of the residual stress (σ_i) of compression in suspended microstructures. **Figure 8**

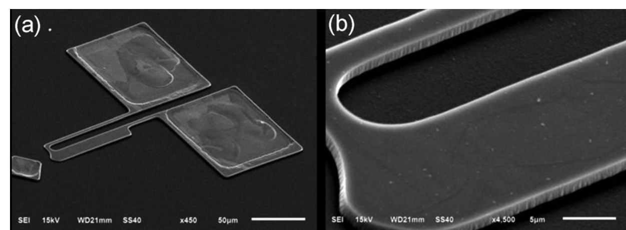

Figure 7: SEM images of the microstructure of a-Si0.50Ge0.50B:H: a) TBA-type microstructure, b) close up of the TBA-type microstructure

Slika 7: SEM-posnetka mikrostrukture a-Si0,50Ge0,50B:H: a) TBA-vrsta mikrostrukture, b) blizu TBA-vrsti mikrostrukture

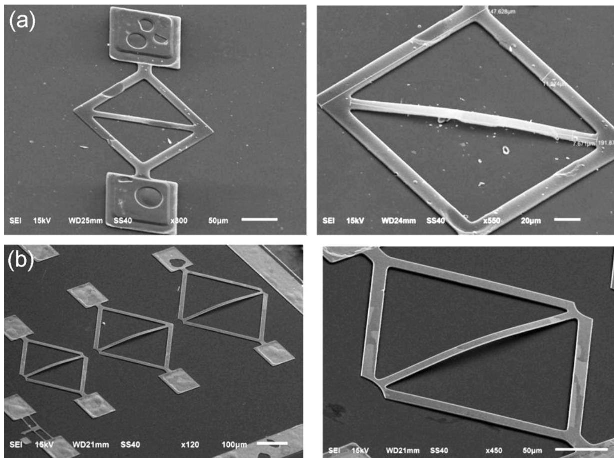

Figure 8: Compression stress ($-\sigma_i$) for diamond-type microstructures: a) microstructure of a-SiB:H, b) microstructure of a-Si0.50Ge0.50B:H
Slika 8: Tlačna napetost ($-\sigma_i$) za diamantno mikrostrukturo: a) mikrostruktura a-SiB:H, b) mikrostruktura a-Si0,50Ge0,50B:H

shows images of diamond-type structures with different lengths and a width of 10 μm across the central bar; the structures present an evident deformation known as the critical length of deformation (buckling), ε_{cr}.

According to Equation 1, the deformation of a-SiB:H diamond-type structures, with a length of 200 μm across the central bar and a width of 10 μm, is 89.363 μm, and the residual stress ($\sigma_i = \varepsilon E$) is calculated to be 13.444 MPa. The a-Si0.50Ge0.50B:H diamond-type structure does not show any lateral chemical attacks, but it indicates a compressive residual stress of 10.661 MPa (**Figure 8**).

Figure 9 shows that the stress is higher when the length of the central bar is smaller; this is because the deformation (ε_{cr}) is directly proportional to the length of the bar and the stress $-\sigma_i$ is directly proportional to the Young's modulus. The Young's modulus of a-Si:H is 160 GPa and for a-Si0.50Ge0.50B:H the Young's modulus is

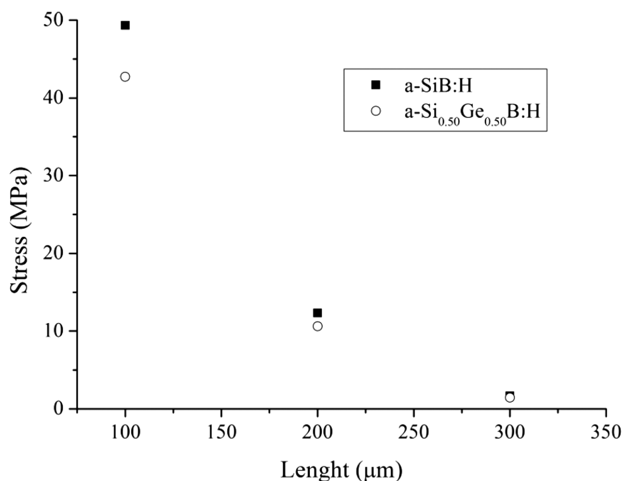

Figure 9: Compression residual stress of diamond-type microstructures versus the length
Slika 9: Zaostale tlačne napetosti pri diamantni mikrostrukturi v odvisnosti od dolžine

130 GPa. So, the a-Si0.50Ge0.50B:H microstructures present less stress.

3 CONCLUSIONS

The work presents the results of manufacturing microstructures with a-SiB:H and a-Si0.50Ge0.50B:H films deposited with a PECVD system at a temperature of 300 °C. The electrical and optical characterization of a-Si1-XGeXB:H thin films was made. The value of the optical gap of the a-SiB:H film is 1.55 eV and for the a-Si0.50Ge0.50B:H film it is 0.97 eV. When germanium content increases, the optical gap decreases rapidly from 1.55 eV to 0.78 eV for a-GeB:H films. The electrical resistance of the a-Si0.50Ge0.50B:H film doped with different concentrations of boron becomes reduced from 6.84 MΩ to 0.56 MΩ. The Young's modulus of amorphous silicon-germanium alloys presents a linear behavior of the silicon/germanium content.

The a-Si0.50Ge0.50B:H suspended microstructures fabricated with a surface micromachining technique at a temperature of 300 °C provide an excellent definition of geometric patterns, having a high mechanical stability in contrast with the microstructures of a-Si1B:H. The advantage of working at low temperatures is a reduction of the residual stress and the intrinsic gradient present at high temperatures. However, diamond-type structures exhibit a compressive mechanical stress of 13.44 MPa for the a-SiB:H structural layer and 10.66 MPa for the a-Si0.50Ge0.50B:H structural layer. We can, therefore, conclude that the microstructures with the a-Si0.50 Ge0.50B:H structural layers deposited at 300 °C using PECVD with the heat treatments < 350 °C can be applied in post-CMOS processes and MEMSs as structural materials. In future we plan to integrate the manufacturing devices and microstructures within a die.

Acknowledgements

The work was supported by Consejo Naciuonal de Ciencia y Tecnología through grant 160164 and by Red Nacional de MEMS.

4 REFERENCES

[1] H. Baltes, O. Brand, A. Hierlemann, D. Lange, C. Hagleitner, CMOS MEMS – present and future, Proc. of the International conference on Micro Electro Mechanical Systems, Las Vegas, 2002, 459–466

[2] S. Beeby, G. Ensell, M. Kraft, N. White, MEMS mechanical sensors, Artech House, Norwood, MA 2004

[3] J. W. Judy, Microelectromechanical systems (MEMS): fabrication, design and applications, Journal of Smart Materials and Structures, 10 (**2001**), 1115–1134

[4] E. K. Petersen, Silicon as a mechanical material, Proceedings of the IEEE, 70 (**1982**), 420–455

[5] J. Stauth, Micromechanical electrostatic resonators in a standard post-CMOS process, UC Berkeley-EECS, 2005, 1–4

[6] F. Yuan, CMOS Current-Mode Circuits for Data Communications, Springer, 2007

[7] J. Laconte, D. Flandre, J. P. Raskin, Micromachined Thin-Film Sensors for SOICMOS Co-Integration, Springer, 2006, 47–103

[8] A. Witvrouw, F. Steenkiste, D. Maes, L. Haspeslagh, P. Gerwen, P. Moor, S. Sedky, C. Hoof, A. Vries, A. Verbist, A. Caussemaeker, B. Parmentier, K. Baert, Why CMOS integrated transducers? A review, Microsystem Technologies, 6 (**2000**), 192–199

[9] T. Hidekuni, S. Kazuaki, I. Makoto, Integrated inductors for RF transmitters in CMOS/MEMS smart microsensor systems, Sensors, 7 (**2007**), 1387–1398

[10] F. Mayer, A. Haberli, H. Jacobs, G. Ofner, H. Baltes, Single CHIP CMOS anemometer, International Electron Devices Meeting, Washington, 1997, 895–898

[11] H. Guckel, D. Burns, C. Rutigliano, E. Lovell, B. Choi, Diagnostic microstructures for the measurement of intrinsic strain in films, J. Micromech, Microeng, 2 (**1992**), 86–95

[12] H. Guckel, T. Randazzo, D. Burns, A simple technique for the determination of mechanical strain in thin films with applications to polysilicon, J. Appl. Phys., 57 (**1985**) 5, 1671–1675

[13] Research Institute. http://www.inaoep.mx/ (accessed 20 April 2010)

[14] G. Craciun, H. Yang, W. Van Zeijl, L. Pakula, A. Blauw, E. Van der Drift, J. French, Single step cryogenic SF6/O2 plasma etching process for the development of inertial devices, Proceedings on semiconductors sensors, Fabrication and characterization, 2002, 612–615

[15] W. Brostow, V. M. Castaño, G. Martinez-Barrera, J. M. Saiter, Pressure-volume-temperature properties of Ge_xSe_{1-x} inorganic polymeric glasses, Physica B, 334 (**2003**), 436–443

[16] F. López, A. Herrera, J. Estrada, C. Zúñiga, B. Cervantes, E. Soto, B. S. Soto-Cruz, Alternative Post-Processing on a CMOS Chip to Fabricate a Planar Microelectrode Array, Sensors, 11 (**2011**), 10940–10957

[17] Software products for engineering simulation, http://www.ansys.com/ (accessed in December 2009)

[18] W. Hernández, I. Zaldivar, C. Zúñiga, A. Torres, C. Reyes, A. Itzmoyol, Optical and compositional properties of amorphous silicon-germanium films by plasma processing for integrated photonics, Optical Materials Express, 2 (**2012**), 358–370

[19] Laboratory Equipments, Available online: http://www.echromtech.com (accessed in September 2011)

[20] B. Nelson, Y. Xu, D. Williamson, D. Han, R. Braunstein, M. Boshta, B. Alavi, Narrow gap a-SiGe:H grown by hot-wire chemical vapor deposition, Thin Solid Films, 430 (**2003**), 104–109

[21] Electronic Instruments, Available online: http://www.keithley.com (accessed in November 2011)

[22] M. Christian, H. Qiuting, A Low-Noise CMOS instrumentation amplifier for thermoelectric infrared detectors, IEEE Journal of Solid-State Circuits, 32 (**1997**), 968–976

[23] I. Toledo, R. Adler, Y. Knafo, O. Kalis, J. Kaplun, BCB etching process using high density plasma, CS MANTECH Conference, Chicago, Illinois, USA, 2008, 14–17

[24] M. Tsai, C. Sun, Y. Liu, C. Wang, W. Fang, Design and application of a metal wet-etching post-process for the improvement of CMOS-MEMS capacitive sensors, Journal of Micromechanics and Microengineering, 19 (**2009**), 1–7

[25] D. Fernández, J. Ricart, J. Madrenas, Experiments on the release of CMOS micromachined metal layers, Journal of Sensors, 2010 (**2010**), article ID 937301, 1–7

[26] P. Merz, H. Quenzer, H. Bernt, B. Wagner, M. Zoberbier, A novel micromachining technology for structuring borosilicate glass substrates, The 12th International Conference on Solid State Sensors, Actuators and Microsystems, Boston, MA, USA, 2003, 258–261

[27] H. Berney, M. Hill, D. Cotter, E. Hynes, M. O'Neill, A. Lane, Determination of the effect of processing steps on the CMOS compatibility of a surface micromachined pressure sensor, Journal of Micromechanics and Microengineering, 11 (**2001**), 402–408

[28] A. Jihwan, V. Brian, Micromachined nerve electrode array integrated with shape memory thin film position clamp, Proceedings of E240, 2007, 1–4

[29] T. Gregory, I. Nadimi, E. Kurt, Bulk micromachining of silicon, Proceedings of the IEEE, 86 (**1998**), 1536–1550

[30] Microresist Technology, Available online: http://www.microresist.de/home_en.htm (accessed in September 2011)